

Self-interaction-corrected local density approximation pseudopotential calculations of the structural phase transformations of ZnO and ZnS under high pressure

This article has been downloaded from IOPscience. Please scroll down to see the full text article.

2000 J. Phys.: Condens. Matter 12 5639

(<http://iopscience.iop.org/0953-8984/12/26/311>)

View [the table of contents for this issue](#), or go to the [journal homepage](#) for more

Download details:

IP Address: 171.66.16.221

The article was downloaded on 16/05/2010 at 05:17

Please note that [terms and conditions apply](#).

Self-interaction-corrected local density approximation pseudopotential calculations of the structural phase transformations of ZnO and ZnS under high pressure

A Qteish

Department of Physics, Yarmouk University, Irbid, Jordan

Received 14 March 2000

Abstract. The structural phase transformations under high pressure of ZnO and ZnS have been investigated by using the Vogel–Krüger–Pollmann (VKP) scheme, in which the electronic self-interaction correction to the local density approximation (LDA) is introduced in a non-self-consistent manner within the pseudopotential approach. In these calculations, I have used highly optimized pseudopotentials and a plane-wave expansion of the wavefunctions. Moreover, the electronic structures of the zinc-blende (ZB) and rock-salt (RS) phases of both compounds have been similarly calculated. It has been found that the VKP scheme provides a highly improved description, relative to the LDA results, for the structural and electronic structure properties of the considered systems. However, the so-calculated transition pressures of the ZB-to-RS transition for both ZnO and ZnS are found to be significantly larger than the experimental data. RS-ZnO is predicted to be an indirect-gap semiconductor, with a wide band gap of 4.2 eV.

1. Introduction

The modern computational methods applied to condensed matter systems are mainly based on density functional theory (DFT) [1]. The major achievement of the Kohn and Sham (KS) formalism [2] of DFT is the *exact* transformation of the many-body problem to a single-body problem. Moreover, the theory itself suggests some workable approximations for the effective single-particle potential. The most widely used is the local density approximation (LDA) for the exchange–correlation (XC) potential. Recently, the generalized gradient approximation (GGA) has been receiving increasing interest [3], and several GGA functionals have been devised. The LDA is found to give surprisingly good results for many physical and chemical properties of a wide range of materials, including the structural phase transformations under high pressure [4]. However, it has several drawbacks. For solids, the general understanding is that the LDA slightly underestimates the lattice parameter and overestimates the cohesive energy and bulk modulus. However, this is not always true and thus cannot be relied upon. The most serious shortcoming is the so-called *band-gap problem*: the LDA band gaps of insulators and semiconductors are about 50% smaller than the corresponding experimental values. The main success of the GGA is a definite improvement in the cohesive energies of solids and molecules. Its performance for other properties, such as lattice parameters and bulk moduli of solids, is not that impressive: the GGA results may even be worse than the LDA ones. As for the electronic structure, the differences between those calculated using the LDA and GGA are marginal.

In the IIB–VI compounds, which are our main concern here, the cation d bands lie within the main valence band, between 7 and 11 eV below the valence band maximum (VBM) [5].

Thus, these semi-core d electrons have significant effects on the basic properties of these compounds. The LDA results for the positions of the d bands are higher than the experimental values by 2 to 3 eV [6]. It is well known that this deficiency results from the spurious self-interaction (SI) [7] allowed by the LDA. Such a shortcoming is found lead to large errors in the calculated [6] band gaps and dispersion of the valence bands, including the d bands themselves. Further errors due to this deficiency are pointed out in reference [7].

Recently, quasi-particle band-structure calculations for IIB–VI compounds have been performed, within the *GW*-approximation, by several groups [8–10]. The band gaps of these materials are well reproduced by these calculations. The binding energies of the semi-core d electrons are also improved, relative to the LDA results, but they are still systematically lower than the experimental values. Zhang *et al* [7] have shown that a good description of the binding energies of the semi-core d electrons can be obtained by using a broken-symmetry approach, based on Slater's 'transition-state' concept. This approach requires large-supercell calculations, so it is quite involved and highly expensive.

The major shortcoming of the LDA and to a lesser extent the GGA is that they allow some spurious SI. It is well known that the SI increases the eigenvalues of the localized orbitals. For example, the LDA eigenvalue of the 1s state of the H atom is about a half of its true value (1 Ryd). Perdew and Zunger have suggested a straightforward method for overcoming this deficiency [11]. Their idea is basically a simple subtraction of the interaction energy of each electron, with its own charge density, from the LDA (or the local spin-density (LSD) approximation) total energy. This SI-corrected LSD (SIC-LSD) scheme leads to orbital-dependent effective potentials which do not preserve the translational symmetry of the Bravais lattice. Therefore, the SIC-LSD calculations are much more difficult than the LSD ones. For this reason, in the self-consistent SIC-LSD calculations [12–14], the SIC is applied *only* to the highly localized states. This SIC-LSD approach has been used to investigate [12–14] the basic properties of transition metals and their oxides, Ce compounds and high- T_c superconductors. These calculations gave an improved description of the structural and electronic structural properties of the materials studied, relative to the LSD results, especially for the latter properties. However, it should be stressed again that these calculations are quite involved and very expensive, and the SIC is applied *only* to the highly localized states.

Recently, an approximate and simple SIC-LDA pseudopotential scheme has been introduced by Vogel, Krüger and Pollmann (VKP) [6]. In this scheme the SIC potentials of the electronic states of solids are approximated by the SIC potentials of the corresponding *atomic* states. Moreover, the latter SIC potentials are incorporated as parts of the ionic pseudopotentials. Hereafter, to distinguish between the VKP scheme and VKP calculations, this scheme will be referred to as the SIC-PP approach. In this way, the translation symmetry of the solid Hamiltonian is preserved and the computational complexity of the SIC-PP scheme is similar to that of the standard LDA calculations. Despite its appealing simplicity, the SIC-PP method is found to substantially correct the LDA-related errors in the band gaps, positions of the d bands, dispersion of the upper three valence bands, position and dispersion of the lowest valence band, lattice parameters and bulk moduli of the IIB–VI compounds [6]. Similar results have also been found for the group-III nitrides [15]. It is worth noting that the VKP calculations were performed by using Bachelet *et al* [16] pseudopotentials, which are quite strong for the highly localized states, and a Gaussian orbital expansion of the solid valence wavefunctions.

On the other hand, the structural phase transformations of semiconductors under high pressure have recently attracted a lot of attention. Recent experiments performed by using image-plate angle-dispersive x-ray techniques for many II–VI, III–V and group-IV semiconductors have significantly altered our understanding of their structural systematics from the view that had been widely accepted [17]. New low-symmetry phases have been observed, such

as: the cinnabar phases in CdTe [18], ZnTe [19] and GaAs [20]; *Cmcm* structure in many II–VI and III–V compounds [17]; the SC16 (simple cubic with a 16-atom basis) form in GaAs [21]. The latter structure has also been observed in CuCl and CuBr [22]. These experimental results have stimulated many theoretical investigations (see, for example, reference [4] and references therein), based on the LDA. These investigations have provided much needed support for and an explanation of these new experimental results, as well as interesting predictions [4]. Some of the newly observed phases have very narrow pressure ranges of stability—such as the cinnabar phase. This means that extremely accurate calculations are required for a meaningful theoretical investigation of the stability of these structures. Therefore, it is very tempting to apply the SIC-PP approach to investigate the structural phase transformations of IIB–VI compounds under high pressure. This approach, which gives very good band gaps, may also solve the problems associated with the artificial metallization of some of the high-pressure phases (in the LDA calculations). Moreover, the relative stability of the different phases of the same compound is very sensitive, so such an application provides a stringent test for the SIC-PP approach.

In this work, I will use the SIC-PP approach to investigate the structural phase transformations of ZnO and ZnS under high pressure. At ambient pressure, ZnS crystallizes in the zinc-blende (ZB) structure, while ZnO crystallizes in the wurtzite (W) form. ZB-ZnO is also known to exist [23], but as a metastable state. Under moderate pressures, W-ZnO and ZB-ZnS transform to the rock-salt (RS) structure. It has been observed that RS-ZnS becomes unstable with respect to the *Cmcm* form at about 65 GPa [17, 24]. Moreover, SC16-ZnS has been predicted to be a stable high-pressure structure [4], with a pressure range of stability below that of RS-ZnS. The W and ZB structures have local tetrahedral bonding and they only differ in second-nearest neighbours. In the case of ZnO, the effects of such a difference on the band gap are found to be quite negligible [9]. I will show, here, that the difference between the calculated transition pressures, p_t , of the ZB \rightarrow RS and W \rightarrow RS transitions of ZnO is also very small. Thus, for the purpose of testing the applicability of the SIC-PP approach for studying the structural phase transformations of the IIB–VI compounds under high pressure, I will focus mainly on the ZB \rightarrow RS transition for both ZnO and ZnS. Moreover, the electronic structures of both the ZB and RS phases of ZnO and ZnS will be calculated (using the LDA and SIC-PP approaches) and discussed in comparison with the available theoretical results and experimental data. The present calculations differ from those of VKP [6] in the sense that, in the present work, I used highly optimized Zn and O pseudopotentials (generated by using the scheme of Lin *et al* [25]) and a plane-wave (PW) expansion of the wavefunctions. The effects of using highly optimized pseudopotentials, in the SIC-PP calculations, will be investigated.

The rest of this paper is organized as follows. In section 2, I will describe briefly the SIC-PP approach and give the computational details. In section 3, I will report and discuss my results for the structural and electronic structure properties of the ZB and RS phases of ZnO and ZnS, and for p_t for the ZB \rightarrow RS transition for both compounds. Finally, a summary of the main results and conclusions will be given in section 4.

2. The SIC-PP approach and computational details

In the SIC-LDA formalism of Perdew and Zunger [11], the total energy of a system of electrons in an external potential is given by

$$E_{tot}^{SIC-LDA} = T_0 + E_{ext} + E_H[n] + E_{XC}^{LDA}[n] - \sum_i^{occ} \left[\frac{1}{2} \int V_H[n_i] n_i(\mathbf{r}) \, d\mathbf{r} + E_{XC}^{LSD}[n_i \uparrow, 0] \right] \quad (1)$$

where: T_0 is the kinetic energy of non-interacting electrons; E_{ext} is the electron interaction energy with the external potential, V_{ext} ; E_H is the classical Coulomb (or Hartree) interaction energy; V_H is the Hartree potential; E_{XC} is the XC energy. Here, n refers to the total electronic charge density, while $n_{i\uparrow}$ corresponds to that of the i th orbital with spin \uparrow . The corresponding single-particle KS equation takes the form (in atomic units)

$$\left[-\nabla^2/2 + V_{ext} + V_H[n] + V_{XC}^{LDA}[n] - V_H[n_i] - V_{XC}^{LSD}[n_{i\uparrow}, 0]\right] \Psi_i^{SIC}(\mathbf{r}) = \varepsilon_i^{SIC} \Psi_i^{SIC}(\mathbf{r}) \quad (2)$$

where V_{XC} is the XC potential. As is evident from equation (2), the SIC-LDA (or SIC-LSD) formalism leads to orbital-dependent effective potentials, which considerably complicate such calculations; see above.

In the SIC-PP approach of VKP [6], the SIC is applied *only* to the valence states. Their main idea is that the orbital-dependent SIC potentials (each the sum of the two potentials which depend on n_i , in equation (2)) can be approximated by that of the corresponding states of the isolated atoms. Moreover, the SIC potentials can be incorporated within the ionic pseudopotentials; see below. The resulting pseudopotentials are used in solid-state calculations in the same way as the LDA ones. Therefore, the effective potential, in the SIC-PP scheme, is orbital independent, and hence the SIC-PP calculations are of the same complexity as the LDA ones.

The major weakness of the SIC-PP approach is that the SIC is incorporated in a non-self-consistent manner. Thus, one expects the accuracy of this approximation to be reduced on going to systems with smaller bond ionicity. This, in fact, has been noticed by VKP in the case of the IIB–VI compounds: the SIC-induced improvements in the electronic structures of the Se- and Te-based compounds are smaller than those for the O- and S-based ones. Moreover, the degree of localization of the valence electrons differs from one crystal structure to another for the same compound, and hence so also does the performance of the SIC-PP approach. The present work touches on this issue. The SIC-LDA pseudopotentials for Zn, O and S used in this work are constructed as follows.

First, norm-conserving LDA pseudopotentials are constructed by using the Kerker scheme [26]. The valence atomic configurations used are $3d^{10}4s^{1.73}4p^{0.27}$ and $2s^22p^4$ for Zn and O, respectively. In the generation of the S pseudopotential, I have used $3s^23p^4$ for the s and p components and $3s^23p^{2.5}3d^{0.5}$ for the d component. The core radii, r_c , used for the s, p and d orbitals, respectively, are: 1.73, 2.11 and 2.01 a_0 for Zn; 0.71 and 1.8 a_0 for O; 1.32, 1.46 and 1.62 a_0 for S. Unless otherwise specified, the results reported were obtained by using pseudopotentials generated with these values for r_c .

Second, the Zn d and O p components of the above-generated pseudopotentials are optimized, by using the scheme of Lin *et al* [25]. This is done by expanding the pseudo-wavefunctions, ψ_l^{PS} , inside the core region in terms of four spherical Bessel functions. The expansion coefficients are, then, adjusted to minimize the kinetic energy beyond a chosen wavevector cut-off, q_c , which is assumed to be equal to q_4 (q for the fourth-order Bessel function). The values of q_c^2 obtained (using the above values for r_c) are about 49 Ryd, for both Zn and O. The optimized ψ_p^{PS} of O is compared with the all-electron and non-optimized ones in figure 1. The similarly optimized ψ_p^{PS} obtained with $r_c = 1.40 a_0$ is also shown in the same figure. A similar comparison for ψ_d^{PS} for Zn can be found in reference [25]. This shows that the optimized wavefunctions ψ^{PS} of these states are more delocalized than the corresponding non-optimized ones, which, in turn, are more extended than the all-electron ones, ψ . Moreover, the degree of localization of the state decreases with increasing r_c . The effects of the change in the degree of localization of the semi-core electrons on the SIC-PP results for structural and electronic structure properties will be discussed in the next section.

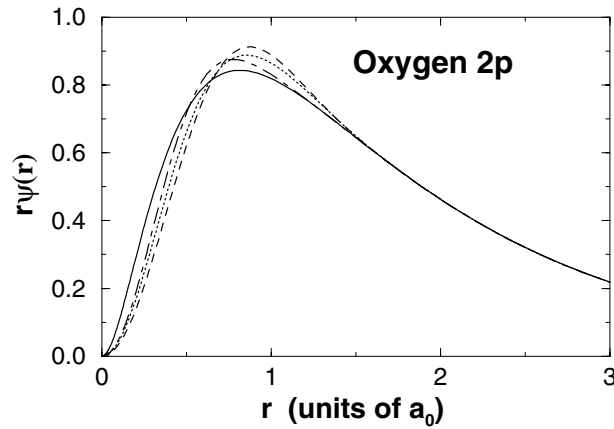


Figure 1. The pseudo-wavefunction of the O 2p state, compared with the all-electron wavefunction (solid line). Dashed line: optimized and with $r_c = 1.8 a_0$. Dotted line: non-optimized and with $r_c = 1.8 a_0$. Dashed-dotted line: optimized and with $r_c = 1.4 a_0$.

Third, the SIC potentials are added to the above-generated LDA ionic pseudopotentials, $V_{ion,l}^{LDA}$, as suggested by VKP [6]. This is done by solving self-consistently the SIC-LDA single-particle Schrödinger equation of the pseudo-atom, or

$$\left\{ -\frac{1}{2}\nabla^2 + V_{ion,l}^{LDA} + V_H[n^v] + V_{XC}[n^v] - V_H[n_l] + V_{XC}^{LSD}[n_{l\uparrow}, 0] \right\} \psi_l^{SIC} = \varepsilon_l^{SIC} \psi_l^{SIC}. \quad (3)$$

Here, the valence states are denoted by their angular momentum l . This is valid only for the non-relativistic calculations, but the generalization to the relativistic calculations can be trivially carried out. After solving equation (3), the SIC-LDA pseudopotentials are defined as

$$V_{ion,l}^{SIC}(r) = V_{ion,l}^{LDA}(r) - V_l^{SIC}(r) \quad (4)$$

with

$$V_l^{SIC} = V_H[n_l] + V_{XC}^{LSD}[n_{l\uparrow}, 0]. \quad (5)$$

As expected, the $V_l^{SIC}(r)$ are long ranged (they have $-1/r$ tails) which is problematic in solid-state calculations. To overcome this difficulty, VKP have suggested the following modifications.

- (i) All of the $V_l^{SIC}(r)$ are rigidly shifted up in energy to make $V_m^{SIC}(r_{loc})$ equal to zero, where m denotes the most extended valence state and r_{loc} is a certain cut-off radius.
- (ii) The $V_l^{SIC}(r)$ are set to zero for $r > r_{loc}$. The value of r_{loc} is chosen to be quite large, in order to ensure that these modifications lead to only a rigid shift in the calculated eigenvalues and that the effects on the calculated wavefunctions are negligible. In this work, I have used the value for r_{loc} suggested by VKP for the Zn-based compounds ($8.34 a_0$).
- (iii) To make the modified $V_l^{SIC}(r)$ go smoothly to zero at r_{loc} , it has been multiplied by a cut-off function of the form $\exp(-(r/r_{loc})^7)$.

Fourth, so that we can use the modified $V_{ion,l}^{SIC}(r)$ in the solid-state calculations, they are separated into local and short-ranged semi-local parts, and the latter parts are then transformed to the separable Kleinman–Bylander (KB) form [27]. Usually, the local part of the pseudopotential, V_{loc} , is chosen to be one of its components (s, p or d). In the VKP calculations [28], the SIC is *not* applied to the component which is chosen as V_{loc} , which is the s and the d component for the cations and the anions, respectively. This means that the

SIC is applied only to the states which form the solid *valence* bands. This choice is justified, since the conduction band states are highly delocalized. Here, I have also adopted the same strategy. However, to avoid ghost states [29], V_{loc} is considered to be the arithmetic average of the s and p components of the corresponding LDA pseudopotentials for both O and S.

If the $V_{ion,l}^{SIC}$ are used in the solid-state calculations, the total energy, forces and stresses must also be corrected for SI. This should be done at the same level of approximation as that of the $V_{ion,l}^{SIC}$. The term giving the correction to the total-energy expression takes the form

$$\Delta E^{SIC} = \sum_l \int V_{E,l}^{SIC}(\mathbf{r}) n_l(\mathbf{r}) d\mathbf{r} \quad (6)$$

where

$$V_{E,l}^{SIC} = \frac{1}{2} V_H[n_l] + V_{XC}^{LSD}[n_{l\uparrow}, 0] - E_{XC}^{LSD}[n_{l\uparrow}, 0]. \quad (7)$$

Here, the $V_{E,l}^{SIC}$ are also shifted, truncated, smoothed and transformed into the KB form in the same manner as $V_{ion,l}^{SIC}(r)$. For more details see reference [6]. The terms giving the correction to the forces on the ions and the stress tensor are nothing but the derivatives of ΔE^{SIC} with respect to the ionic position and strain tensor, respectively.

Only three crystal structures have been considered, in this work, namely ZB, RS and W. The first two structures can be fully defined by just the lattice parameter, a . The latter phase is a hexagonal structure (with two formula units per primitive unit cell) which can be described by three structural parameters: a , c and an internal parameter, u . The optimal values of c/a and u for each of the volumes of W-ZnO considered were determined by minimizing the stress anisotropy and the forces on the ions, respectively.

The other computational details are as follows. PWs up to a 55 Ryd energy cut-off were used to expand the wavefunctions of the phases considered for both ZnO and ZnS. Such a cut-off is found to give very good total-energy convergence for ZnS [4]. So that we can use the same cut-off for ZnO, r_c for the O 2p orbital is chosen in such a way that the value obtained for q_c is very close to that for Zn 3d; see above. The Kohn–Sham equations were solved by using the conjugate-gradient methods of references [30] and [31]. For the LDA and LSD exchange–correlation potentials, I have used the Ceperley–Alder [32] data, as parametrized by Perdew and Zunger [11]. The integration over the Brillouin zone was done by using a regular $4 \times 4 \times 4$ Monkhorst and Pack [33] mesh in all cases, and all the systems considered were treated as semiconductors. In the LDA calculations, the RS phase of ZnO is an indirect-band-gap semiconductor, while that of ZnS is a semimetal; see below. However, for the latter system the VBM and conduction band minimum (CBM) occur at different places, and so it is more appropriate to treat it as a semiconductor (in the LDA calculations). The use of the above mesh has also been checked before and is found to provide an excellent convergence [4].

3. Results and discussion

3.1. Structural parameters and relative stability

The structural parameters of the structures of ZnO and ZnS considered are determined by calculating E_{tot} at six or seven different volumes, V , around the equilibrium one, and fitting the results obtained to the Murnaghan equation of state. For W-ZnO, the optimal values of c/a and u have been determined for each of the values of V considered, as described above.

In figure 2, I show the fitted E_{tot} -versus- V curves for the phases of ZnO and ZnS considered, obtained by using the LDA and SIC-PP approaches. The LDA results for the E_{tot} -versus- V curve of ZB-ZnO are slightly higher (by 0.003 eV/atom near the equilibrium

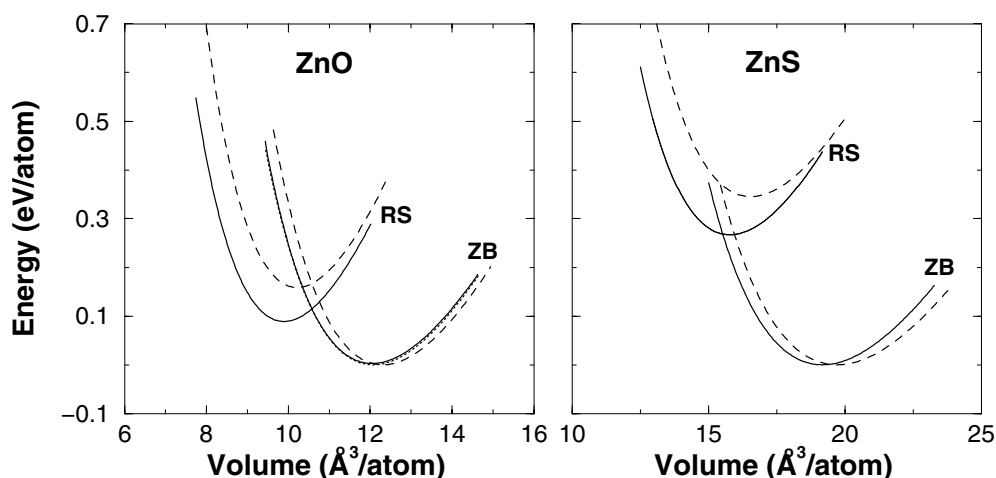


Figure 2. Energy-versus-volume curves of the ZB and RS phases of ZnO and ZnS. Solid lines: LDA calculations; dashed lines: SIC-PP calculations. That of W-ZnO obtained from LDA calculations is also shown (dotted line).

volume) than those for the W structure. This finding is in agreement with the fact that the latter phase is the ground-state structure of ZnO. However, the energy difference between these two curves is too small to lead to an appreciable difference between the transition pressures, p_t , of the ZB \rightarrow RS and W \rightarrow RS transitions of ZnO (see table 3, later). This justifies the choice of the former transition in studying the SIC-induced effects for ZnO. The most important feature to note, from figure 2, is the large difference, in the LDA and SIC-PP results for the relative stability, between the ZB and RS phases for both ZnO and ZnS. The LDA results for the difference in ground-state energy E_{tot} of the RS and ZB phases of ZnO and ZnS are 0.086 and 0.267 eV/atom, respectively, whereas the corresponding SIC-PP results are 0.159 and 0.345 eV/atom. The discrepancies between the LDA and SIC-PP results have a large influence on the calculated values of p_t for the ZB \rightarrow RS transitions of ZnO and ZnS; see section 3.3. For an explanation of such differences see also section 3.3.

The calculated structural parameters of the phases of ZnO and ZnS considered are listed in table 1, compared with the available experimental data and other theoretical results. The important features to note are the following.

First, the LDA results for the equilibrium lattice parameters (a_{eq}) are systematically smaller than the corresponding SIC-PP ones. This trend is consistent with the results obtained by VKP [6] for many IIB–VI compounds. However, the averaged SIC-induced increases in value of a_{eq} are smaller than those reported in reference [6]: about 2.4%, compared to about 1% in the present calculations. It is worth noting that the latter value is comparable to the usual LDA underestimation of a_{eq} .

Second, the SIC-induced changes in the calculated values of the bulk modulus at the equilibrium volume (B_{eq}), in the present calculations, do not show a clear trend: the SIC-PP values are larger than the LDA ones for the ZB and RS phases of ZnO, and the reverse is true for the structures of ZnS considered. Interestingly, these changes are in the right direction, except for RS-ZnS. However, the SIC-PP value of B_{eq} for RS-ZnS is still in excellent agreement with experiment (note the large error bar on the experimental value). These results are not consistent with those of VKP [6], where it was found that the SIC-PP results are always smaller than the LDA ones. Moreover, the magnitudes of the SIC-induced changes in the values of B_{eq} are also

Table 1. The structural parameters of the phases of ZnO and ZnS considered. The LDA results for the phases of ZnS considered were previously reported in reference [4].

System	Structural parameters			
		LDA	SIC-PP	Experiment
W-ZnO	a_{eq} (Å)	3.261 ^a , 3.23 ^b	3.29 ^b	3.2496(6) ^c
	c_{eq} (Å)	5.242 ^a , 5.18 ^b	5.29 ^b	5.2042(20) ^c
	B_{eq} (GPa)	151.9 ^a , 160 ^{b,c}	159 ^b	183 ^c , 143 ^d
	B'_{eq}	4.681 ^a , 4.4 ^c	—	4 (fix)
	u	0.380 ^a , 0.381 ^c	—	0.3820(8) ^d
ZB-ZnO	a_{eq} (Å)	4.585 ^a	4.618 ^a , 4.596 ^e	4.62 ^f
	B_{eq} (GPa)	152.9 ^a	162.6 ^a , 164.1 ^e	
	B'_{eq}	4.984 ^a	4.700 ^a , 4.436 ^e	
RS-ZnO	a_{eq} (Å)	4.294 ^a	4.340 ^a , 4.322 ^e	4.271(2) ^c
	B_{eq} (GPa)	197.7 ^a , 205 ^c	216.3 ^a , 217.6 ^e	228(7) ^c
	B'_{eq}	4.434 ^a , 4.88 ^c	4.773 ^a , 4.300 ^e	4 (fix) ^c
ZB-ZnS	a_{eq} (Å)	5.352 ^a , 5.25 ^b	5.402 ^a , 5.42 ^b	5.413(13) ^c
	B_{eq} (GPa)	83.1 ^a , 101 ^b	80.6 ^a , 81 ^b	76.0(2.0) ^c
	B'_{eq}	4.43 ^a	4.31 ^a	4 (fix) ^c
RS-ZnS	a_{eq} (Å)	5.017 ^a	5.097 ^a	5.060(15) ^c
	B_{eq} (GPa)	104.4 ^a	100.0 ^a	104(6) ^c
	B'_{eq}	4.28 ^a	4.55 ^a	4 (fix) ^c

^a Present work, using the Zn, S and O pseudopotentials adopted.

^b Reference [6].

^c Reference [34].

^d Reference [35].

^e Present work, using Zn and O pseudopotentials generated with small values for r_c ; see the text.

^f Reference [23].

significantly smaller than those reported in reference [6]: about 17%, on average, compared to 6% in the present calculations.

Third, there are some discrepancies between the results of the present LDA and SIC-PP calculations and those of VKP for both a_{eq} and B_{eq} . The maximum differences are in the LDA results of ZB-ZnS, which are about 2% and 20% for a_{eq} and B_{eq} , respectively. However, considering the differences between the computational ingredients of the present and the VKP calculations (see above), the agreement between the results of these calculations, generally speaking, is quite reasonable.

Fourth, both the LDA and SIC-PP values of a_{eq} for the phases of ZnO considered are slightly larger than the experimental data, except for ZB-ZnO. One might argue that this may be due to the use of optimized pseudopotentials with quite large core radii for the Zn 3d and O 2p orbitals; see above. This is true to some extent: the SIC-PP values are reduced by about 0.4%—see table 1—when the calculations are performed by using optimized Zn and O pseudopotentials generated with r_c equal to 1.6 and 1.4 a_0 for the Zn 3d and O 2p wavefunctions, respectively. These calculations were performed by using a 90 Ryd energy cut-off, which is found to give an excellent convergence. The above reduction in the calculated values of a_{eq} is roughly equal to the errors in the present LDA results.

Fifth, the SIC-PP results for both a_{eq} and B_{eq} are, generally speaking, in better agreement with experiment than the LDA ones. This means that the SIC-PP approach provides equations of state which are quite superior to those of the LDA, which, in principle, should lead to a

better description of the structural phase transformations under high pressure. Unfortunately, we will see below that this is not the case.

3.2. Electronic structure

In this subsection I will only report and discuss the band structures of the ZB and RS phases of both ZnO and ZnS, calculated by using the LDA and SIC-PP approaches. The ZB and RS structures have the same Bravais lattice, which allows for an easy and direct check of the transferability of the SIC-induced effects on the electronic structure of such compounds, by going from one crystal structure to another.

The band structures of the ZB phase of ZnO and ZnS, calculated by using the LDA and SIC-PP approaches, are shown in figures 3 and 4, respectively. The calculated band gaps, positions of the d bands and valence bandwidths of these systems are listed in table 2. For comparison, the other available theoretical results and experimental data are also given in the same table. This table shows that, for both systems, all of these properties are very well reproduced by the SIC-PP calculations, and that the SIC-PP results are in much better agreement with experiment than the LDA ones. This is not the case for the valence bandwidth of ZnO. However, for this quantity, the present SIC-PP result is consistent with the *GW*-calculations [9]; see table 2. The large difference between these theoretical results and experiment was not expected and is difficult to explain. Generally speaking, the present SIC-PP results are consistent with the results obtained similarly by VKP [6].

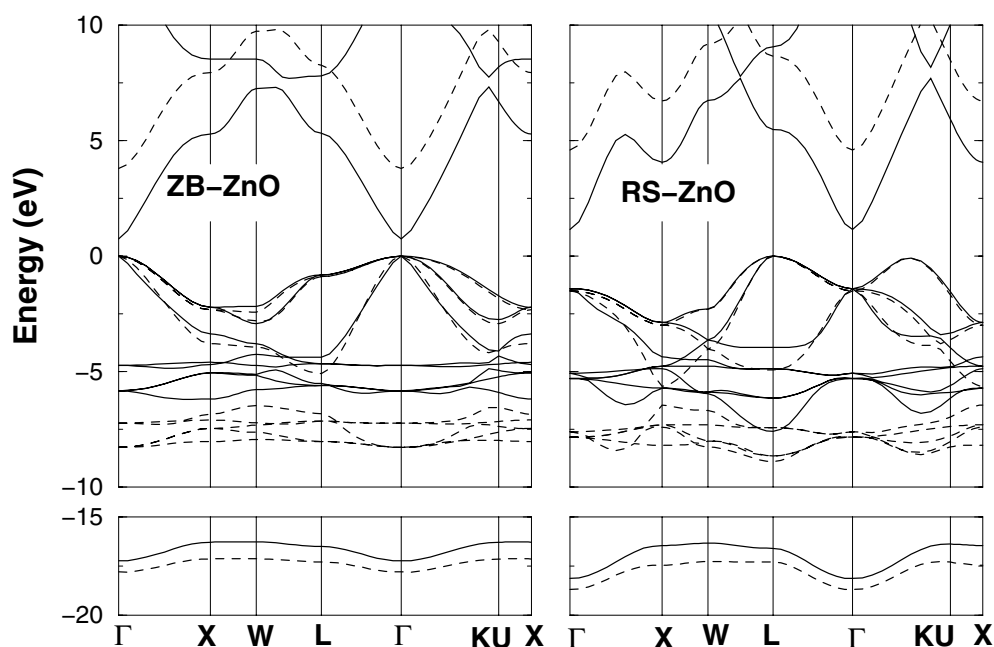


Figure 3. The calculated band structures of the ZB and RS phases of ZnO. Solid lines: LDA calculations; dashed lines: SIC-PP calculations. The zero of energy is chosen to be at the valence band maximum (at the Γ and L points for the ZB and RS phases, respectively).

The electronic structures of the RS phase of ZnO and ZnS are also shown in figures 3 and 4. The remarkable feature to note is that the SIC-induced effects on the electronic structure are transferable to a very large extent: for both compounds considered, the SIC-induced shifts

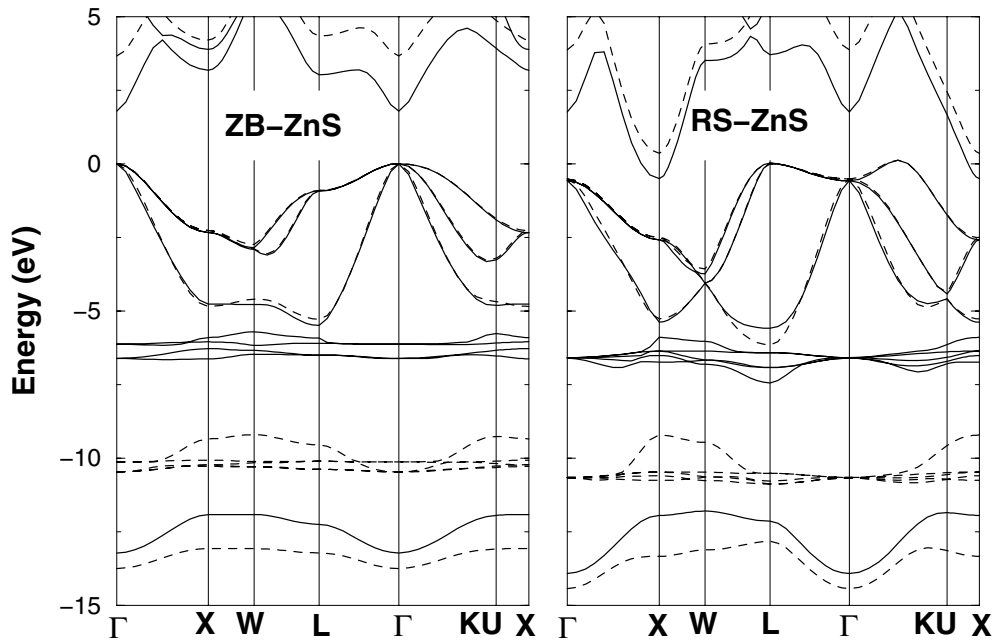


Figure 4. As figure 2, but for ZnS. For RS-ZnS the valence band maximum is along the Γ -K direction.

Table 2. Calculated energy gaps (E_g), averaged positions of the Zn d bands (E_d) relative to the valence band maximum and valence bandwidths (VBW) of the ZB phase for ZnO and ZnS, compared with the experimental data. ‘SIRC-PP’ denotes SIC-PP calculations which take into account the effects of the relaxation of the Zn d electrons; see reference [6]. For ZnO, the experimental results and those of reference [6] are for the wurtzite structure. All listed values are in units of eV.

System	Electronic property	Present work		Reference [6]			Reference [9]		Experiment
		LDA	SIC-PP	LDA	SIC-PP	SIRC-PP	LDA	<i>GW</i>	
ZnO	E_g	0.75 ^a	3.75 ^a , 3.95 ^b	0.2	3.8	3.5	1.1	3.6	3.4 ^c
	E_d	-5.4 ^a	-7.8 ^a , -8.66 ^b	-5.0	-8.9	-7.5	-5.3	-6.6	~ -7.8 ^c
	VBW	17.2 ^a	17.8 ^a	—	—	—	17.4	17.9	~ 25 ^d
ZnS	E_g	1.8 ^a	3.7 ^a	2.0	3.4	3.7	1.9	4.0	3.8 ^c
	E_d	-6.4 ^a	-10.3 ^a	-5.9	-11.4	-9.4	-6.6	-8.4	~ -10 ^c
	VBW	13.2 ^a	13.75 ^a	—	—	—	13.1	13.1	13.5 ^c

^a Using the Zn, S and O pseudopotentials adopted.

^b Using Zn and O pseudopotentials generated with small values for r_c ; see the text.

^c Reference [35].

^d Reference [39].

in the energy bands of the ZB and RS phases, and the changes in their dispersion, are very similar. This finding and the fact that the electronic structures of the ZB and W phases of ZnO are very similar [9] suggest that the SIC-induced changes in the electronic structure of W-ZnO, which is not considered in this work, would be extremely close to the ones found for ZB-ZnO.

Another important feature to note, from figures 3 and 4, is that the SIC-induced shifts of the bands, relative to each other, are not rigid, but are combined with important changes in the

dispersion of these bands, compared to the LDA results. This is most notable for the upper three valence bands of the phases of ZnO considered. For ZB-ZnO, the LDA and SIC-PP values for the widths of these bands are 4.38 and 5.07 eV, respectively. These results are consistent with those of VKP (4.0 and 5.2 eV, respectively). Moreover, the SIC-PP results in both the present and VKP calculations are in good agreement with the experimental value of 5.3 eV. It is worth noting that the experimental results and those of VKP are for W-ZnO. There are three factors which contribute to the SIC-induced changes in the band dispersion:

- (i) The position dependence of the SIC potentials included.
- (ii) The shifts in the positions of the bands relative to each other change the degree of the mixing (hybridization) between them: in particular, (a) the symmetry-allowed p–d [5] hybridization between the Zn d levels and the upper three valence band states (which are mainly derived from the anion p states) and (b) the s–d hybridization [36] with the lowest valence band states (which originate from the anion s states), away from the Γ point. In the LDA calculations, the d bands of the phases of ZnO considered overlap with the upper valence bands, which wrongly enhances the p–d mixing between their states. This is largely corrected in the SIC-PP calculation, where the d bands are pushed down in energy and separated from the upper valence bands. As a result, the dispersions of the upper valence bands are substantially improved; see above. On the other hand, the increase in the binding energies of the semi-core d electrons enhances the s–d hybridization. This is reflected in the quite large dispersion (in the SIC-PP calculations) of the uppermost d band for both RS and ZB phases of ZnS, since it has the same symmetry as the lowest valence band, away from the Γ point.
- (iii) The increase in the degree of localization of the electrons in the SIC-PP calculations. This is responsible for the decrease in the width of the lowest valence band and the d bands (except the uppermost one), especially in the case of the two phases of ZnS considered.

It is important to note, from table 2, that the present SIC-PP results for the averaged positions of the d bands, for both ZnO and ZnS, are about 1 eV higher than the corresponding VKP results [6], and that the present results are in excellent agreement with experiment. This can be understood as a consequence of using optimized pseudopotentials in the present work. It has been shown, in section 2, that the pseudopotential optimization decreases the localization of the semi-core electrons, which, in turn, leads to a reduction in their SIC. To show that this is the case, I have performed band-structure calculations by using the optimized Zn and O pseudopotentials generated with rather small values for r_c (see subsection 3.1). The results are also given in table 2. The so-obtained SIC-PP value for the averaged position of the d bands of ZB-ZnO is -8.66 eV, which is significantly closer to the corresponding result of VKP (-8.9 eV) than the value obtained by using the Zn and O pseudopotentials adopted in this work (-7.8 eV). It is worth noting that the SIC-PP band gap of ZB-ZnO is also affected by this process (increased from 3.75 to 3.95 eV). This can be understood as due to the further downshift of the upper valence bands (due to the increase of localization of the O 2p states) and the reduction in strength of the p–d hybridization, caused by the further increase in the binding energies of the d electrons. However, one should be careful when comparing the calculated binding energies of the semi-core d electrons with the experimental photoemission values, since the latter include electronic relaxation effects. In fact, VKP [6] found that their SIC-PP results become in much better agreement with experiment upon including the electronic relaxation effects; see table 2. The agreement between the present SIC-PP results and experiment is achieved by using highly optimized pseudopotentials. Thus, the effects of using these pseudopotentials are comparable to those of the electronic relaxation, for the systems considered.

Finally, from figures 3 and 4, one observes that the SIC-induced upward shift of the lowest conduction band, relative to the LDA results, has a quite significant dependence on the wavevector (k) for the phases of ZnS considered, whereas this is not the case for those of ZnO. To understand these results, we should recall that the SIC is applied only to the valence states. Therefore, the SIC-induced effects on the lowest conduction band are *indirect*, and the opening of the band gap in the SIC-PP calculations is mostly due to a downward shift of the uppermost valence bands. Moreover, the lowest conduction band of ZnO, relative to the VBM, is higher than that of ZnS, on average, by about 2 eV. Thus, the indirect SIC effects on the lowest conduction band for ZnO should be smaller than those for ZnS, which explains the above results. Furthermore, the application of the SIC to the conduction band states is not expected to appreciably alter this picture. The upward shift of the lowest conduction band and its k -dependence have important implications for the fundamental band gaps of the RS phase for both ZnO and ZnS. In the former system, the lowering of the lowest conduction band at the X point, on going from the ZB to the RS phase, is not enough to make this point the position of the CBM. So, RS-ZnO is an indirect-band-gap semiconductor, with the VBM at the L point and the CBM at the Γ point. The direct band gap of ZB-ZnO, at the Γ point, is 3.75 eV: about 0.35 eV higher than the experimental value. Thus, this indicates that RS-ZnO has a quite large indirect band gap of about 4.2 eV. This value is larger than the direct band gap, at the Γ point, of ZB-ZnO, which increases under the application of external pressure. Interestingly, the above-predicted value is much larger than the value of 1.36 eV suggested by Jaffe *et al* [37], based on Hartree–Fock calculations. Unfortunately, to the best of my knowledge, no experimental measurements of the band gap of RS-ZnO are available yet. However, there is an indirect indication [34] that this system is non-metallic. New experimental investigations of the electronic structure of the W, ZB and RS forms of ZnO are highly desirable. As for RS-ZnS, the SIC-induced upward shift of the conduction band at the X point is 0.9 eV, compared to that at the Γ point of 2.1 eV. Thus, according to the SIC-PP calculations, RS-ZnS is an indirect-gap semiconductor with a band gap of 0.24 eV, which is much smaller than the experimental value of about 2 eV (from reference [38]).

3.3. Structural phase transitions under high pressure

For the reason discussed above, I will concentrate here on the ZB \rightarrow RS phase transition of ZnO and ZnS. p_t is determined from the constraint of equal static lattice enthalpy, given by

$$H(p) = E_{tot}(V(p)) + pV(p). \quad (8)$$

The $H(p)$ calculated for the RS phases of ZnO and ZnS, relative to those of the corresponding ZB structures, obtained by using the LDA and SIC-PP approaches, are shown in figure 5. The values obtained for p_t are listed in table 3, compared with the other theoretical results and experimental data. The interesting features to note are the following.

- (i) The LDA values of p_t for the ZB \rightarrow RS phase transition for both ZnO (6.6 GPa) and ZnS (14.35 GPa) are in excellent agreement with the experimental results (between 2.0 and 8.7 GPa [34] and about 15 GPa, respectively). These experimental results for ZnO were obtained [34] upon pressure increase and decrease, respectively, and they correspond to the pressures when half the sample has transformed.
- (ii) The SIC-PP values of p_t for the above transition for ZnO and ZnS (13.3 and 21.1 GPa, respectively) are significantly higher than the corresponding experimental data. Therefore, in spite of its success in providing an excellent description of the equation of state and electronic structure for the phases considered for both ZnO and ZnS, the SIC-PP scheme is inappropriate for investigating the structural phase transformations under high pressure.

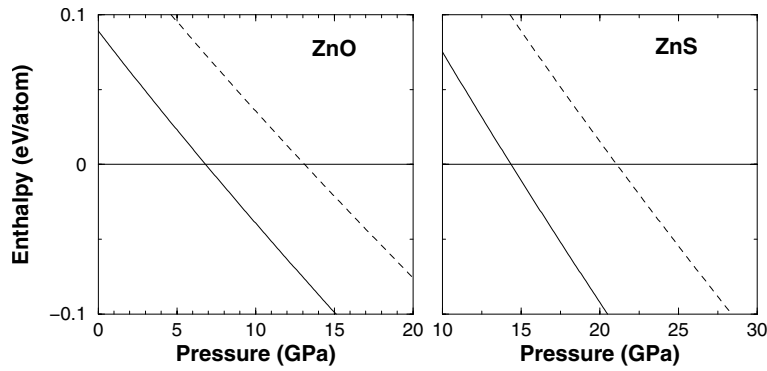


Figure 5. The static lattice enthalpy of the RS phase, relative to that of the corresponding ZB structure for ZnO and ZnS. Solid lines: LDA calculations; dashed lines: SIC-PP calculations.

Table 3. Transition pressures (GPa) of the phase transitions of ZnO and ZnS studied.

System	Transition	Present work		Experiment
		LDA	SIC-PP	
ZnO	ZB \rightarrow RS	6.6 ^a	13.3 ^a , 13.4 ^b	—
	W \rightarrow RS	6.7 ^a	—	2.0–8.7 ^c , 8.0 ^d , 9.0 ^e , 9.5 ^f
ZnS	ZB \rightarrow RS	14.35 ^a	21.1 ^a	14.7–15.4 ^g , 15.0–16.2 ^h , 12.0 ⁱ , 18.1 ^d

^a Using the Zn, S and O pseudopotentials adopted.

^b Using Zn and O pseudopotentials generated with small values for r_c ; see the text.

^c Reference [34].

^d Reference [40].

^e Reference [41].

^f Reference [42].

^g Reference [35].

^h Reference [43].

ⁱ Reference [24].

The overestimation of p_t in the SIC-PP calculations is a direct consequence of the large increase in the relative stability of the ZB and RS phases in such calculations, relative to that of the LDA; see figure 1. The latter discrepancy can be understood as follows. In the SIC-PP scheme, the SIC potentials are assumed to be those of the corresponding atomic states, so they are the same for the two structures. Since the RS phase has smaller volume than the corresponding ZB one, the valence electrons are more delocalized in the former phase and, hence, the SIC-PP scheme is expected to work better for the latter structure. In other words, the valence electrons in the ZB phase benefit more from the presence of the SIC potentials (in the present case) than those of the RS phase. Therefore, the overestimation of p_t in the SIC-PP calculations is an artifact of this approach, in which the SIC is included in a non-self-consistent manner. This is because the energy differences between competing crystal structures are very sensitive quantities.

- (iii) The use of optimized pseudopotentials has very small effects on the calculated values for p_t . The SIC-PP value of p_t for the ZB \rightarrow RS transition of ZnO is increased by 0.1 GPa (see table 3) when the calculations are performed with the Zn and O pseudopotentials generated with rather small values for r_c ; see subsection 3.1.

4. Conclusions

The simple SIC-LDA pseudopotential (SIC-PP) scheme recently introduced by Vogel, Krüger and Pollmann (VKP) is used, in conjunction with optimized pseudopotentials and a plane-wave expansion of the wavefunctions, to calculate the structural and electronic structure properties of the zinc-blende (ZB) and rock-salt (RS) phases of both ZnO and ZnS. Furthermore, the ZB \rightarrow RS phase transition of these two compounds has also been similarly investigated. The main results and conclusions can be summarized as follows.

- (i) The SIC-PP approach provides a highly improved description for the electronic structure and equation of state of the phases considered for both ZnO and ZnS, over the LDA results, especially for the former properties.
- (ii) The SIC-induced effects on the electronic structures of the ZB and RS phases are very similar, for both ZnO and ZnS.
- (iii) Despite these findings, the SIC-PP scheme is found to be inappropriate for investigating the structural phase transformations under high pressure.
- (iv) The optimization of the pseudopotentials leads to a decrease in the SIC-PP values for the binding energies of the semi-core electrons, making the so-obtained results in very good agreement with the experimental data.
- (v) The SIC-induced upward shift of the lowest conduction band is found to have a quite strong wavevector dependence for the phases of ZnS considered, while this is not the case for those of ZnO. As a result, the SIC-PP value for the indirect band gap of RS-ZnS is much smaller than the experimental data, although the band gap of ZB-ZnS is well reproduced by these calculations.
- (vi) RS-ZnO is predicted to be an indirect-band-gap semiconductor with a large band gap of 4.2 eV.

Acknowledgments

The work was done within the framework of the Associateship Scheme of the Abdul-Salam International Centre for Theoretical Physics, Trieste, Italy. I am indebted to Abdullah I Al-Sharif, Dirk Vogel, Jörg Neugebauer and Martin Fuchs for stimulating discussions.

References

- [1] Hohenberg P and Kohn W 1964 *Phys. Rev.* **136** B864
- [2] Kohn W and Sham L J 1965 *Phys. Rev.* **140** A1133
- [3] See for example, Fuchs M, Bockstede M, Pehlke E and Scheffler M 1998 *Phys. Rev. B* **57** 2134 and references therein
- [4] Qteish A and Muñoz A 2000 *J. Phys.: Condens. Matter* **12** 1705
Qteish A and Parrinello M 2000 *Phys. Rev. B* **61** 6521
- [5] Wei S-H and Zunger A 1988 *Phys. Rev. B* **37** 8958
- [6] Vogel D, Krüger P and Pollmann J 1996 *Phys. Rev. B* **54** 5495
- [7] Zhang S B, Wei S-H and Zunger A 1995 *Phys. Rev. B* **52** 13 975
- [8] Rohlfing M, Krüger P and Pollmann J 1998 *Phys. Rev. B* **57** 6485
- [9] Oshikiri M and Aryasetiawan F 1999 *Phys. Rev. B* **60** 10 754
- [10] Zakharov O, Rubio A, Blase X, Cohen M L and Louie S G 1994 *Phys. Rev. B* **50** 10 780
- [11] Perdew J P and Zunger A 1981 *Phys. Rev. B* **23** 5048
- [12] Svane A and Gunnarsson O 1990 *Phys. Rev. Lett.* **65** 1148
- [13] Szotek Z, Temmermann W M and Winter H 1993 *Phys. Rev. B* **47** 4029
- [14] Arai M and Fujiwara T 1995 *Phys. Rev. B* **51** 1477
- [15] Vogel D, Krüger P and Pollmann J 1997 *Phys. Rev. B* **55** 12 836

- [16] Bachelet G B, Hamann D R and Schlüter M 1982 *Phys. Rev. B* **26** 4199
- [17] Nelmes R J and McMahon M I 1998 *Semiconductors and Semimetals* vol 54 (New York: Academic) p 145
- [18] McMahon M I, Nelmes R J, Wright N G and Allan D R 1993 *Phys. Rev. B* **48** 16 246
- [19] Nelmes R J, McMahon M I, Wright N G and Allan D R 1995 *J. Phys. Chem. Solids* **56** 545
- [20] McMahon M I and Nelmes R J 1997 *Phys. Rev. Lett.* **78** 3697
- [21] McMahon M I, Nelmes R J, Allan D R, Belmonte S A and Bovornratanaraks T 1998 *Phys. Rev. Lett.* **80** 5564
- [22] Hull S and Keen D A 1994 *Phys. Rev. B* **50** 5868
- [23] Bragg W H and Darbyshire J A 1954 *J. Met.* **6** 238
- [24] Desgreniers S, Beaulieu L and Lepage L 2000 *Phys. Rev. B* **61** 8726
- [25] Lin J S, Qteish A, Payne M C and Heine V 1993 *Phys. Rev. B* **47** 4174
- [26] Kerker G P 1980 *J. Phys. C: Solid State Phys.* **13** L189
- [27] Kleinman L and Bylander D M 1982 *Phys. Rev. Lett.* **48** 1425
- [28] Vogel D, private communications
- [29] Gonze X, Käckell P and Scheffler M 1990 *Phys. Rev. B* **41** 12 264
- [30] Teter M P, Payne M C and Allen D C 1989 *Phys. Rev. B* **40** 12 255
- [31] Qteish A 1995 *Phys. Rev. B* **52** 1830
- [32] Ceperley D M and Alder B J 1980 *Phys. Rev. Lett.* **45** 566
- [33] Monkhorst H J and Pack J D 1976 *Phys. Rev. B* **13** 5189
- [34] Karzel H *et al* 1996 *Phys. Rev. B* **53** 11 425
- [35] *Landolt-Börnstein New Series* 1987 Group III, vol 22a, ed K-H Hellwege and O Madelung (Berlin: Springer)
- [36] Fiorentini V, Methfessel M and Scheffler M 1993 *Phys. Rev. B* **47** 13 353
- [37] Jaffe J E, Pandey R and Seel M J 1991 *Phys. Rev. B* **43** 14 030
- [38] Ves S, Schwarz U, Christensen N E, Syassen K and Cardona M 1990 *Phys. Rev. B* **42** 9113
- [39] Ley L, Pollak R A, McFeely F R, Kowalczyk S P and Shirley D 1974 *Phys. Rev. B* **9** 600
- [40] Samara G A and Drickamer H G 1962 *J. Phys. Chem. Solids* **23** 457
- [41] Jamieson J C 1970 *Phys. Earth Planet. Inter.* **3** 201
- [42] Bates C H, White W B and Roy R 1962 *Science* **137** 993
- [43] Piermarini G J and Block S 1975 *Rev. Sci. Instrum.* **46** 973
- Yu S C, Spain I L and Skelton E F 1978 *Solid State Commun.* **25** 49
- Yagi T and Akimoto S 1976 *J. Appl. Phys.* **47** 3350
- Onodera A and Ohtani A 1980 *J. Appl. Phys.* **51** 2581